Acta of Bioengineering and Biomechanics
Vol. 23, No. 4, 2021

Original paper
DOI: 10.37190/ABB-01947-2021-04

Study on nonlinear constitutive model of skin under compression load over a wide range of strain rates

XIAOPING ZHANG[1], CUN WEN[1], CHENGLI TANG[1], SUSU LIU[1]*, YAOKE WEN[2], YAPING WANG[2], ZHENYU BAO[2], SHAOMIN LUO[3]

[1] School of Mechanical Engineering, Nantong University, Nantong, China.
[2] School of Mechanical Engineering, Nanjing University of Science & Technology, Nanjing, China.
[3] School of Aerospace Engineering, Guizhou Institute of Technology, Guiyang, China.

Purpose: In wound ballistics, skin has obvious blocking effect in the biological target penetration of projectiles. An analytical description of skin mechanical properties under compression can set the basis for the numerical simulation and the evaluation of blocking effect. *Methods*: In this study, an improved three-parameter solid visco-elastic model was proposed to describe the skin creep phenomenon. And then combined with Maxwell and Ogden model, a new nonlinear skin constitutive model, consisting of hyper-elastic unit, creep unit and relaxation unit in parallel, was established. Here, we examine the material properties of freshly harvested porcine skin in compression at strain rates from 0.01/s to 4000/s. *Results*: The model is verified by comparison with the experimental results by our test and that in the literature at different strain rates. *Conclusions*: It shows that calculated results of the constitutive model agree well with the experiment data at extremely low to high strain rates, which is useful for the description of the heterogeneous, nonlinear viscoelastic, relaxation and creep mechanical response of skin under compression.

Key words: *constitutive model, pig skin, three-parameter solid model, Maxwell, creep phenomenon*

1. Introduction

Skin is the outermost layer of the body and acts as a first protective barrier against external agents such as light, heat, infection, and injury. In wound ballistics, the blocking effect of skin on projectiles has been concerned in the research, such as penetration threshold velocity [7], [24], [33] and skin wound morphology [8], [9], [16]. However, the above-mentioned factors are insufficient to evaluate the blocking effect of skin because of the difference of skin, and assessing it by researching the mechanical properties and constitutive model of skin could be an effective method.

At present, a large amount of experiment has been devoted to the mechanical characterization of the skin in various biomedical areas. In 1966, Ridge et al. [28] first conducted the uniaxial experiment on excised skin which showed skin's anisotropy. Then, in 1974, Lanir and Fung [19] established an experimental setup for the tests of rabbit skin which can perform two-dimensional relaxation and stretch tests. After that, Schneider et al. [30] used the same setup for the characterization of excised human skin in 1984. Afterwards, a few studies based on the uniaxial and biaxial experiments has shown that the properties of skin is nonlinear, anisotropic, and viscoelastic (time-dependent) [1], [27], [29]. Due to the discovery of strain rate sensitivity of skin by Finlay [10] earlier in 1970, the different strain rate experiments of skin have attracted the attention of many researchers. According to high and low speed tensile failure experiments of rat skin, Haut RC [13]

* Corresponding author: Susu Liu, School of Mechanical Engineering, Nantong University, Nantong 226019, China. E-mail: liususu1006@139.com
Received: October 3rd, 2021
Accepted for publication: January 3rd, 2022

observed that the tensile failure properties depend on location, orientation, age and strain rate. In 1989, Wu et al. [35] found that the Poisson ratio of pig skin is dependent on the loading and strain rate in 2003. The uniaxial compressive experiments were conducted by Shergold in 2006 [31] at low strain rates and high strain rates which were performed using a split Hopkinson pressure bar, showing that pig skin has a bigger strain rate sensitivity compared to silicone rubbers which are regarded as skin substitution. Application of SHPB is effective extremely to measure the compressive mechanical response of skin at high strain rates. In order to measure the tensile respond of skin under dynamic loading, Lim et al. [22] modified a SHTB to conduct the dynamic experiments which also show the rate sensitive, orthotropic, and non-linear behavior of pig skin. In addition, a great many researchers [18], [25], [32] took dynamic shear tests which show the highly nonlinear viscoelastic behavior, and Soetens et al. [32] developed a constitutive model that capture the experimentally observed strain stiffening, softening and increasing viscous dissipation. In summary, based on the mechanical respond of the skin, it showed that skin is an anisotropic, non-linear elastic material that exhibits viscoelasticity and loading history dependence.

For the mechanical properties of skin, many researchers have proposed a constitutive model to represent these properties. Hyperelastic model is a currently used skin constitutive model, which is a strain energy density function model developed on the basis of rubber model and can describe the hyperelastic response of skin. Shergold et al. [31] compared the Ogden and Mooney–Rivlin model by the uniaxial compressive experiments of silicone rubber and pig skin and found that the latter is unable to describe solids with a strong strain hardening characteristic. The Ogden hyperelastic model was also regarded as the suitable choice to define the nonlinear mechanical behavior of skin tissue in tension [15], [17], [20]. However, in order to fully characterize the mechanical behavior of skin under impact, its viscoelastic properties must also be determined [11]. Holt et al. [14] established a viscoelastic constitutive model to describe the mechanical properties of human skin under low shear loads, which can describe the strain hardening phenomenon of skin. Soetens et al. [32] established a visco-hyperelastic model of human skin under oscillating shear with large amplitude, which can accurately capture the phenomena of nonlinear viscous dissipation between skin. In addition, some scholars tried to establish semi-structural models which take into account the constituents of the material and include their respective mechanical behaviors, and potentially their relative interactions. Weiss et al. [34] proposed a transversely anisotropic hyperelastic model of collagenous tissues for the description of ligaments, accounting for the uncrimping process of collagen fibers. This formulation was later adapted for skin by Groves et al. [12] in an attempt to fit their data on uniaxial tensile tests on human and murine skin.

As the research moves along, single viscoelastic and hyperelastic models are not enough to characterize the mechanical properties of skin. Note that more complete representations of skin's behavior can be obtained by coupling different constitutive models [26]. Therefore, it is absolutely imperative that establishing a coupling constitutive model which considers different respond of skin. In this study, considering the skin strain rate sensitivity, nonlinear viscous dissipation and relaxation and creep phenomenon, a relatively complete phenomenological model of skin is proposed to describe its stress–strain response under compression. Here, we examine the material properties of freshly harvested porcine skin in compression at strain rates in the range of 0.01/s–4000/s and verify this constitutive model based on the experimental results which include our experiment data and cited literature about pig skin. This study establishes a material constitutive model for skin which can be used as a reference to research the blocking effect of skin substitutes and mimics in the field of wound ballistics hopefully.

2. Materials and methods

2.1. Experimental setup

Pig skin was investigated to avoid the ethical issues associated with testing human skin and pig skin is one of the substitute materials for studying human skin due to its similarity in material response to human skin. In addition, the thickness of the human and pig dermis is similar: for human skin, the dermis thickness ranges from 1mm on the face to 4 mm on the back [31], whilst the dermis of the pig varies from 1 to 6 mm in thickness. In addition, by contrast with *in vivo* measurements, the excised experimentation usually ensures a better control of the boundary conditions and eliminate the effect of muscle under the skin.

We have done the mechanical tests about pig skin from the belly of landrace (Parallel to the direction of spine) in the previous research [2]. After the residual

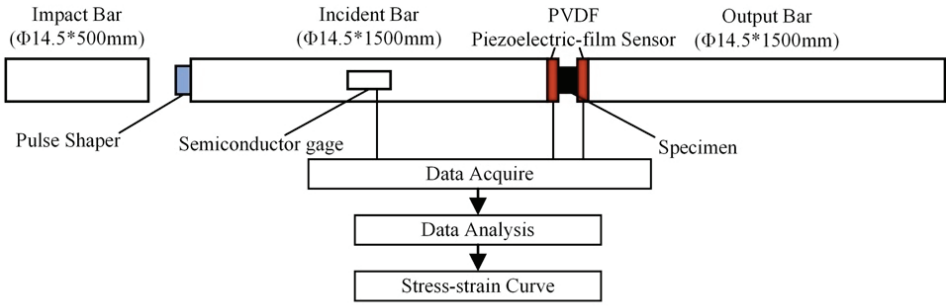

Fig. 1. Schematic representation of the SHPB

fat on the hypodermis was removed, the cylindrical specimens were cut using a corneal ring. The pig skin specimens were submerged in Krebs–Ringer solution for storage before the tests. Soft tissue remains active for more than two weeks when placed in Krebs–Ringer solution without significant changes in mechanical properties [6].

Quasi-static compression tests were carried out in an MTS universal testing. Samples were tested at different strain rates ranging from 0.01/s to 0.1/s. Right cylinders with dimensions of 2.5 mm in thickness and 20 mm in diameter were used. A sketch of the SHPB used for measuring the compressive uniaxial stress versus strain response of pig skin, at strain rates of between 2000/s and 4000/s, is given in Fig. 1. A low specimen aspect ratio was chosen to minimize the time required to reach force equilibrium along the axis of the specimen in the high strain rate compression tests. Previous studies using a SHPB indicate that the constraint on the specimen is negligible for aspect ratios within the range of 0.25–0.5 [5]. The specimens for high strain rate tests are 8 mm in diameter and the same thickness as in low strain rate tests (2.5 mm), as shown in Fig. 2.

Fig. 2. Cylindrical specimens [2]

2.2. Constitutive models

Table 1. Symbols and meanings

Notations	
θ_i	relaxation time
k_i	elastic coefficient of elastic element
η_i	sticky coefficient of sticky pot
ε	strain
$\dot{\varepsilon}$	strain rate
σ	stress
σ_h	the stress obtained by the hyper-elastic unit
σ_c	the stress obtained by the creep unit
σ_v	the stress obtained by the viscoelastic unit
A_n, B_n	coefficient of the model
λ	elongation in the current configuration
μ, α	constant determined by Ogden model

2.2.1. Relaxation unit

A Generalized Maxwell Model is an arrangement in series or in parallel of viscous and elastic components, usually mimicking the microscale arrangement of constituents within the material [3]. There are three common representations: the Maxwell, the Kelvin–Voigt, and the standard models, in which the Maxwell model is suitable for describing the stress relaxation and linear deformation processes of viscoelastic materials, but not for the creep and cross-linking process of materials, while the Kelvin model is exactly the opposite of the Maxwell model. The main feature of skin viscoelasticity is the effect of previous deformation; the stress state depends on the strain or strain rate histories and the relaxation phenomenon caused by viscoelasticity is extremely uniform. Then, in order to accurately describe the stress relaxation phenomenon of the skin, the Maxwell model can be used as the skin relaxation unit [23], as illustrated in Fig. 3 and Eq. (1):

$$\sigma_v = k_1 \int_0^t \dot{\varepsilon}(\tau) e^{-\frac{t-\tau}{\theta_1}} d\tau \,, \tag{1}$$

in which, σ_v denotes the stress, $\dot{\varepsilon}$ – the strain rate, t – the time, θ_1 – the relaxation time, which can be determined the sticky coefficient of η_1,

$$\eta_1 = k_1\theta_1 . \tag{2}$$

Elimination of θ_1 from Eqs. (1) and (2) yields

$$\sigma_v = k_1 \int_0^t \dot{\varepsilon}(\tau) e^{\frac{k_1}{\eta_1}(\tau - t)} d\tau , \tag{3}$$

in which η_1 is the sticky coefficient of sticky pot.

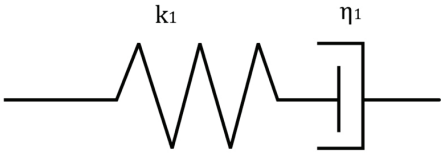

Fig. 3. Generalized Maxwell model

2.2.2. Creep unit

Due to the limitations of the Maxwell and Kelvin models, an improved three-parameter solid model was proposed to express the creep phenomenon caused by skin viscoelasticity, as illustrated in Fig. 4.

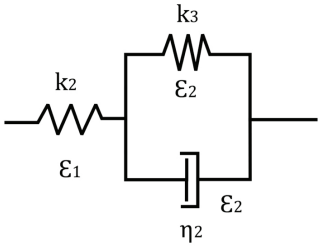

Fig. 4. Three-parameter solid model

For this model, a linear elastic element in parallel with the ideal viscous element was added. For the linear elastic element, its stress–strain relation can be described:

$$\sigma_{c3} = \sigma_{c3}(\varepsilon_2) = k_3\varepsilon_2 , \tag{4}$$

in which, k_3 is the elastic modulus.

For the ideal viscous element, its viscous respond can be described:

$$\sigma_{c2} = \eta_d \frac{d\varepsilon_2}{dt} , \tag{5}$$

in which, η_2 is the coefficient of viscosity.

For this modified model, its stress and strain can be described, respectively:

$$\sigma_c = \sigma_{c1} = k_2\varepsilon_1, \quad \sigma_{c1} = \sigma_{c2} + \sigma_{c3} , \tag{6}$$

$$\varepsilon = \varepsilon_1 + \varepsilon_2 , \tag{7}$$

where $\dot{\varepsilon}$ is the strain rate, ε is the strain, σ_c is the stress obtained by the creep unit.

Substituting in Eqs. (4)–(7), it can be integrated as:

$$\frac{d\varepsilon}{dt} = \frac{1}{k_2}\frac{d\sigma_c}{dt} + \frac{\sigma_c}{\eta_2} - k_3\frac{\varepsilon_2}{\eta_2} , \tag{8}$$

$$\varepsilon_2 = \varepsilon - \frac{\sigma_c}{k_2} , \tag{9}$$

$$\eta_2\dot{\sigma}_c + (k_2 + k_3)\sigma_c = k_2k_3\varepsilon + k_2\eta_2\dot{\varepsilon} . \tag{10}$$

Therefore, based on Eq. (10), the proposed three--parameter solid model is given by:

$$\sigma_c = e^{-\frac{k_2+k_3}{\eta_2}t}\left(\int_0^t \frac{k_2(k_3\varepsilon + \eta_2\dot{\varepsilon})}{\eta_2} e^{\frac{k_2+k_3}{\eta_2}} dt + C\right), \tag{11}$$

in which, C is a constant.

2.2.3. Constitutive model

In order to describe the creep and relaxation phenomena caused by viscoelasticity, strain rate sensitive and nonlinear viscous dissipation, it was assumed that the constitutive equation is composed of hyper-elastic unit, creep unit and relaxation unit in parallel. In the proposed visco-hyperelastic model, Ogden hyper-elastic model was adopted as the hyper-elastic unit, Maxwell model (Eq. (3)) as the relaxation unit, and the proposed three-parameter solid model (Eq. (10)) as the creep unit, as shown in Fig. 5.

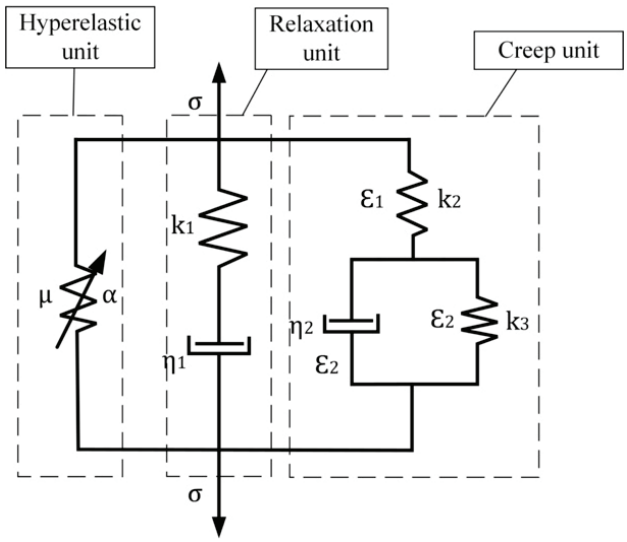

Fig. 5. Constitutive model diagram

The creep deformation is the deformation that increases with time when the load remains constant [21]. At the same strain, the low strain rate takes much longer time than the high strain rate. The lower the strain rate, the smaller the loading rate and the slower the stress change until the stress approximately remains unchanged. So, it is reasonably assumed that the creep deformation is more obvious at low strain rate than that at high strain rate and the creep unit is negatively correlated with the strain rate. A polynomial equation can be introduced to describe the strain rate sensitivity in the constitutive equation, as shown in Eqs. (11) and (12). With the reduction of the influence of creep unit and little change of the influence of relaxation unit, the effect of Maxwell unit is to get bigger and bigger. Then, the total stress of the skin can be expressed as:

$$f_v(\dot{\varepsilon}) = \sum_1^n A_n \dot{\varepsilon}^n, \tag{12}$$

$$f_c(\dot{\varepsilon}) = \frac{1}{\sum_1^n B_n \dot{\varepsilon}^n}, \tag{13}$$

$$\sigma = \sigma_h + f_v(\dot{\varepsilon})\sigma_v + f_c(\dot{\varepsilon})\sigma_c, \tag{14}$$

in which σ denotes the stress, σ_h is the stress obtained by the hyperelastic unit, σ_c is the stress obtained by the creep unit, σ_v is the stress obtained by the viscoelastic unit, A_n and B_n is the coefficient of the model. Moreover, for an incompressible, isotropic, hyper-elastic solid is used here to describe the constitutive behavior of rubber and skin. In one term, Ogden model, the strain energy function takes the form [31]:

$$W = \frac{2\mu}{\alpha}(\lambda_1^\alpha + \lambda_2^\alpha + \lambda_3^\alpha - 3), \tag{15}$$

where α is a strain hardening exponent and μ has the interpretation of the shear modulus under infinitesimal straining.

The specimen is considered to be in a state of plane stress during a uniaxial compression test. For a Cartesian co-ordinate system, with the z-axis aligned with the loading direction, we can write

$$\sigma_x = \sigma_y = 0, \quad \lambda_2 = \lambda_3. \tag{16}$$

The solid is taken as incompressible and so the principal stretch ratios are related by

$$\lambda_x = \lambda_y = \frac{1}{\lambda_z}. \tag{17}$$

Now, it can be specialized to the case of an Ogden strain energy density function (14). This gives:

$$\sigma_h = \frac{2\mu}{\alpha}(\lambda^{\alpha-1} - \lambda^{-1-(\alpha/2)}), \tag{18}$$

in which λ is elongation, μ and α are constants.

Submitting Eq. (3), Eq. (11) and Eq. (18) and assuming $n = 1$, Eq. (13) can be integrated as

$$\sigma = \frac{2\mu}{\alpha}(\lambda^{\alpha-1} - \lambda^{-1-(\alpha/2)}) + A_1\dot{\varepsilon}k_1\int_0^t e^{\frac{k_1}{\eta_1}(\tau-t)}d\tau$$
$$\frac{1}{B_1\dot{\varepsilon}}e^{-\frac{k_2+k_3}{\eta_2}t}\left(\int_0^t \frac{k_2(k_3\varepsilon+\eta_2\dot{\varepsilon})}{\eta_2}e^{\frac{k_2+k_3}{\eta_2}t}dt + C\right). \tag{19}$$

To evaluate the error between model and experimental data at each strain rate, the maximum error rate was calculated according to the formula:

$$E_{\max} = \max\left\{\left|\frac{\sigma_i - \sigma_{mi}}{\sigma_i}\right|\right\}, \tag{20}$$

where σ_i is the real value of the experimental stress, σ_{mi} is the theoretical value of the stress on the basis on models.

3. Results

3.1. Experimental results

In Figure 6, the quasi-static compression stress–strain behavior of pig skin in terms of the true stress and true strain at low strain rates of 0.01/s and 0.1/s and high strain rates of 2000/s, 3000/s and 4000/s are shown. The curves show that the stress–strain response of the pig skin is non-linear with a J-shape. With the rapid increasing of strain rate, the stress also increases sharply, the skin exhibits a significant strain rate effect. The experiments reveal that these soft solids strain harden strongly at high compressive strains.

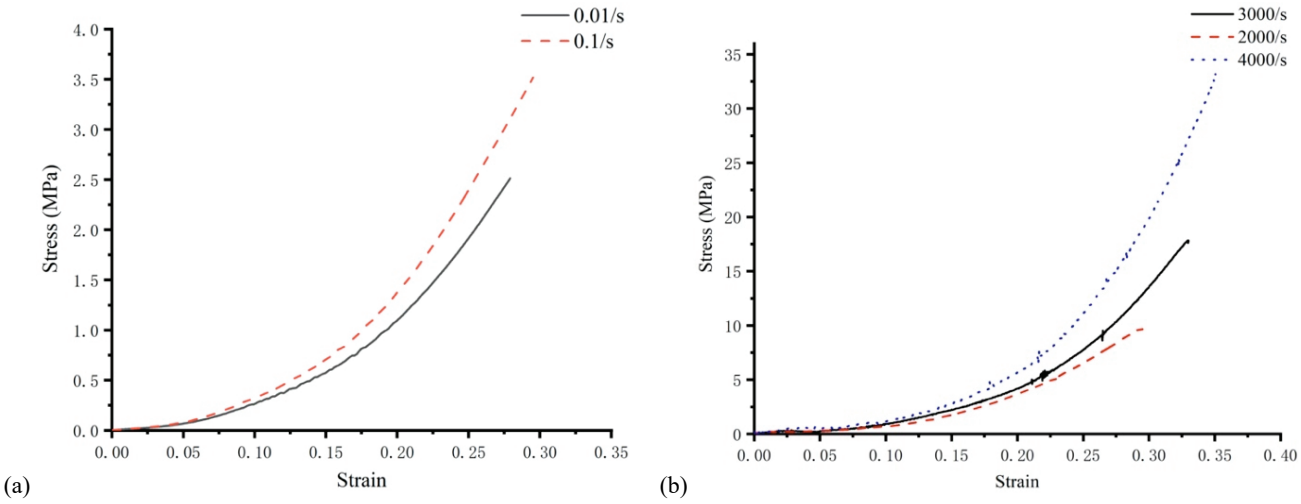

Fig. 6. Stress–strain curve [2]: (a) low strain rates, (b) high strain rates

3.2. Model verification

Five experimental stress–strain results at extremely low strain rates from 0.01/s to 0.1/s and high strain rates from 2000/s to 4000/s were used to verify the constitutive model, reflecting the compression mechanical response characteristics of pig skin from the belly of landrace (Parallel to the direction of spine). The iterative parameter estimation method had a high rate of convergence and resulted in a unique solution for a wide range of initial parameter values [32]. The fit parameters in the constitutive model (Eq. (18)) are identified by iterative parameter estimation method, as listed in Table 2. The maximum error rates are listed in Table 3.

In Figure 7, the compressive stress–strain curves fitted with the constitutive model at quasi-static and high strain rate are represented. It is obvious that the constitutive model can describe the rate effect of pig skin, in which the yield stress increases with the strain rate. Furthermore, the model is in good agreement with the experimental results.

The compressive experimental results of pig skin were cited by Butler et al [4] to verify the constitutive model. The skin samples were excised from the rump of the animal. The constitutive model established constants evaluated using Eq. (18) are given in Table 4 for each strain rate considered. The maximum error rates are listed in Table 5.

The compressive stress–strain responses of the pig skin referenced and fitted are shown in Fig. 8 for a range of strain rates for porcine skin. Each line indicates the result of a single sample test, with each color corresponding to a particular strain rate.

To further prove the applicability of the constitutive model, the compressive experimental results of pig buttock skin made by Shergold et al. [31] were cited, which was obtained using the universal material testing machine at low to medium strain rates and using a SHPB at high strain rate. The parameters of the constitutive model involved in Eq. (18) could be determined based on the pig skin tested results, as shown in Table 6. The maximum error rates are listed in Table 7.

Table 2. Parameters identified in the constitutive model based on experimental results

μ (MPa)	α (–)	k_2 (MPa)	k_3 (MPa)	η_2 (–)	η_1 (–)	k_1 (MPa)	B_1 (–)	A_1 (–)	C (–)
0.0992	1.2776	–8.2568	–0.0156	1.0087	2.65e-5	1.2655	–50.841	–1.95e-4	0.1298

Table 3. The maximum error rates

Strain rates	0.01/s	0.1/s	2000/s	3000/s	4000/s
Maximum error rates	4.3%	9.4%	14.1%	11.1%	4.4%

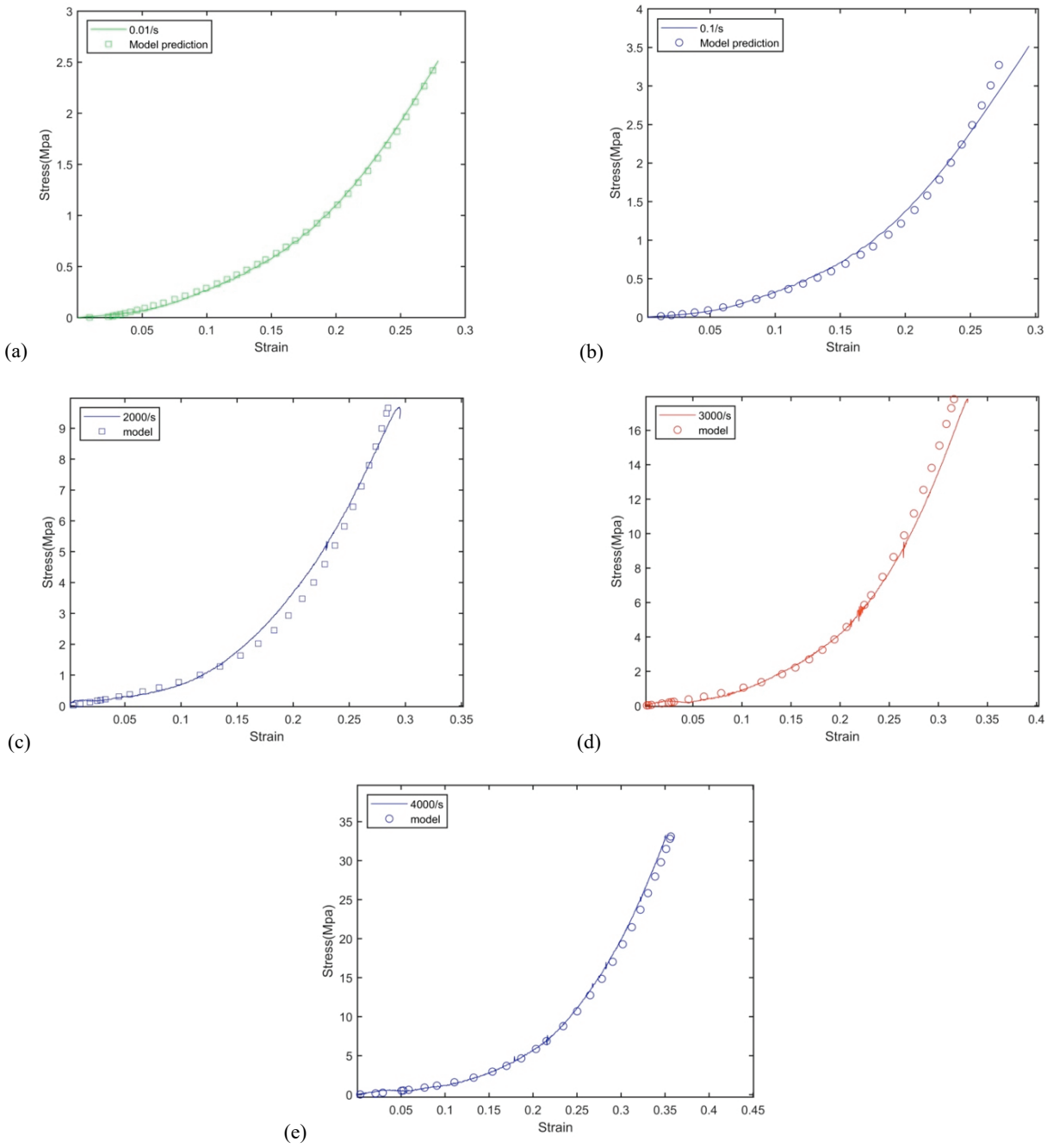

Fig. 7. Comparison between theoretical and experimental results [2] for pig skin in unconfined compression at strain rate equal: (a) 0.01/s, (b) 0.1/s, (c) 2000/s, (d) 3000/s, (e) 4000/s

Table 4. Parameters identified in the constitutive model based on experimental results

μ (MPa)	α (–)	k_2 (MPa)	k_3 (MPa)	η_2 (–)	η_1 (–)	k_1 (MPa)	B_1 (–)	A_1 (–)	C (–)
0.2065	1.2768	–1.01e-5	–1.48e-4	–0.9758	–0.8203	–0.8135	0.7352	0.2620	3.48e-4

Table 5. The maximum error rates

Strain rates	0.01/s	0.1/s	1/s
Maximum error rates	6.3%	12.5%	11.8%

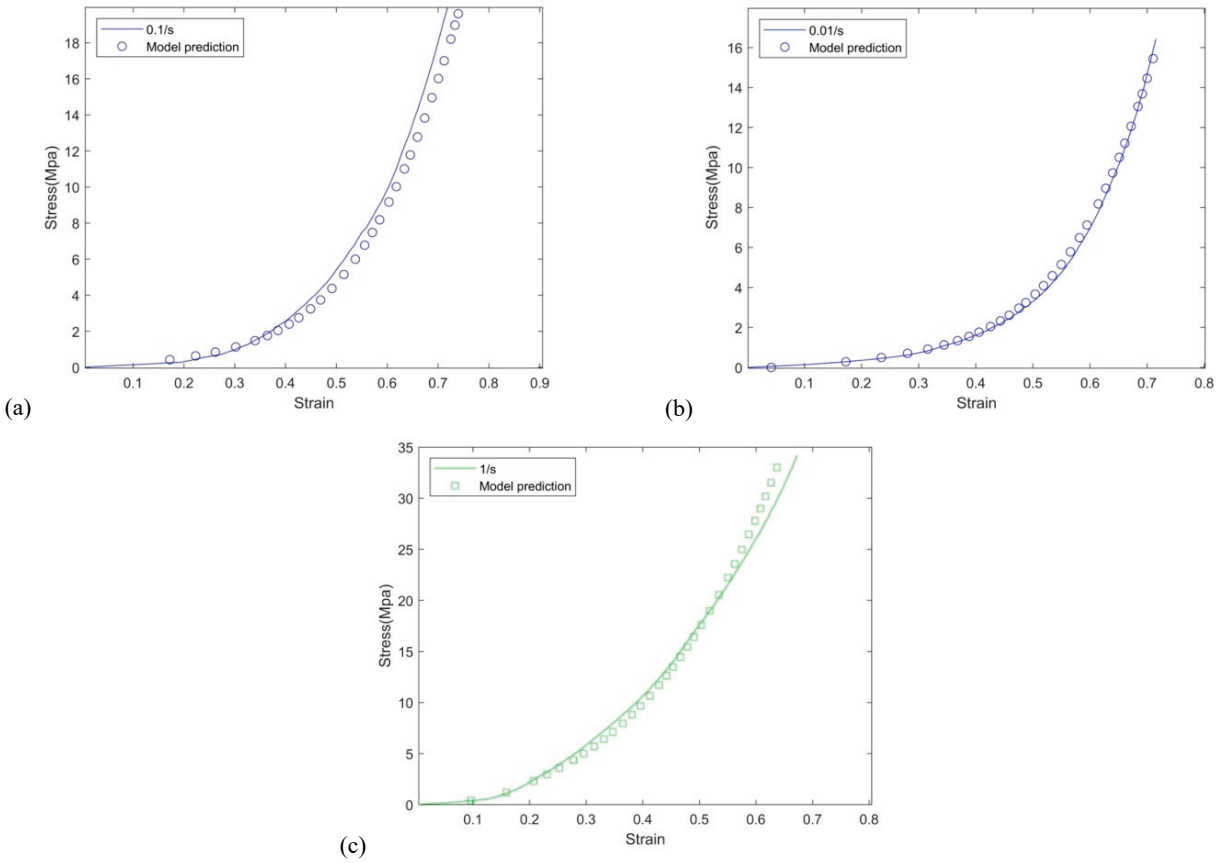

Fig. 8. Comparison between theoretical results and experimental results cited from Butler et al. [4] for pig skin at strain rate equal to: (a) 0.01/s, (b) 0.1/s, (c) 1/s

Table 6. Parameters identified in the constitutive model based on experimental results

μ (MPa)	α (–)	k_2 (MPa)	k_3 (MPa)	η_2 (–)	η_1 (–)	k_1 (MPa)	B_1 (–)	A_1 (–)	C (–)
0.1435	1.2152	39.6888	0.0010	0.0657	2.19e-4	2.0656	33.9351	–-4.25e-5	49.6484

Table 7. The maximum error rates

Strain rates	0.004/s	0.4/s	40/s	4000/s
Maximum error rates	12.8%	6.8%	4.6%	4.5%

The related comparison at low to high strain rates is shown in Fig. 9. It can be seen that the calculated results of the model exhibit closer agreement with the cited experimental results at the tested strain rates. However, there is little experimental data at every strain rate and further verification is needed.

4. Discussion

A large amount of literature has been devoted over decades to the mechanical characterization of the skin, but there is few research about compression test about skin which have been mentioned above can be used for reference. The experimental data cited by Benjamin and Shergold are obtained from same species as our test but different parts. Moreover, it is well known that skin, like any biological material, once removed from its host begins to degrade [21]. Due to these different conditions, three groups of experimental data were fitted separately. As shown in Figs. 7–9, in the case of pig skin, the constitutive model can capture specimen behavior well over a wide range of strain rates.

It is known that a typical stress–strain curve for skin exhibits non-linear behavior, and its response is gen-

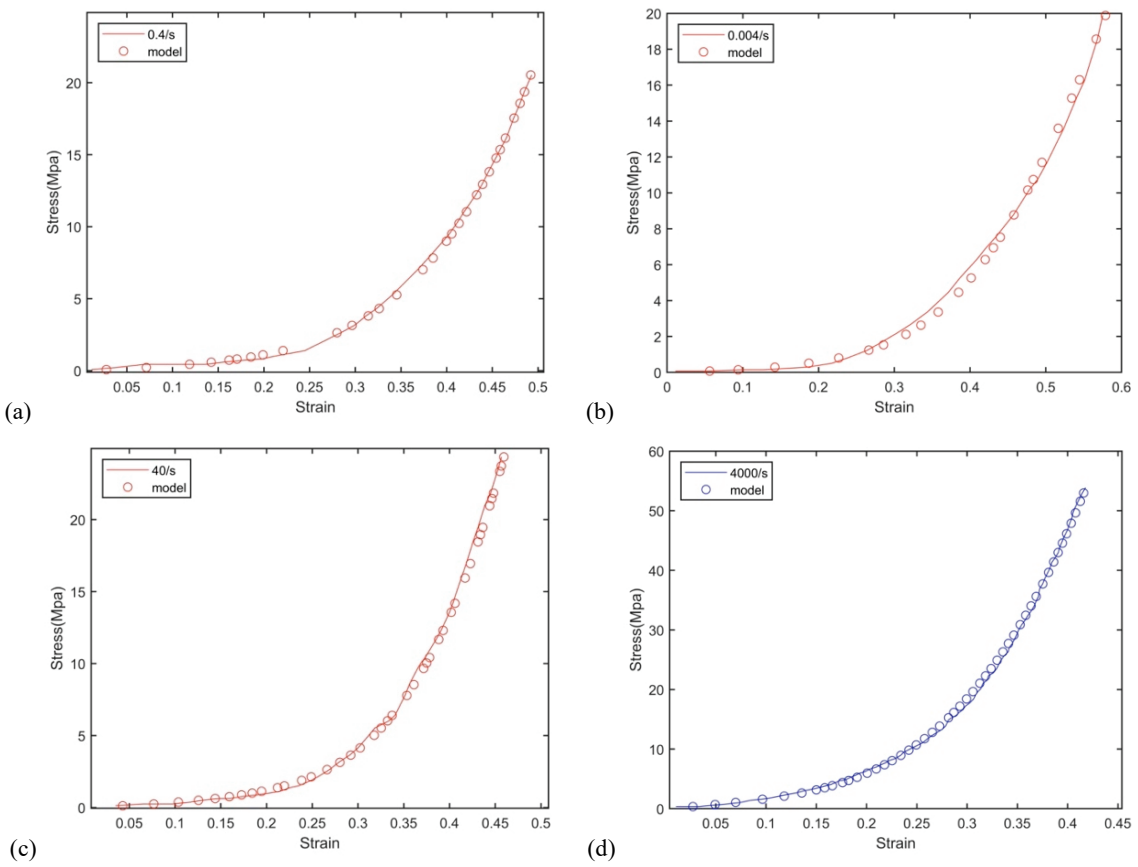

Fig. 9. Comparison between theoretical results and experimental results cited from Shergold et al. [31] for pig skin at strain rate equal to: (a) 0.004/s, (b) 0.004/s, (c) 40/s, (d) 4000/s

erally classified into three stages. In the initial stage, at the beginning of loading, skin is very compliant and large deformation occurs and the fibers are largely unaligned. In the second stage, the stiffness of skin gradually increases as the applied load increases and the stress increases rapidly as the strain increases equably. In the third stage, the relationship between stress and strain gradually becomes linear approximately as the strain continues to increase [11]. In this phase, the collagen fibers predominantly bear the load and provide the skin with a high strength, preventing damage and postponing the eventual skin failure. Obviously, at the end of curve, there is a gap between the fitting results and experimental data. As the load increases, a significant strain hardening is observed for the skin specimens. This transition cannot adequately be captured using these forms of analytical models.

As the constitutive model established including hyper-elastic unit, relaxation unit and creep unit shows, the effect of creep unit declines and the effect of relaxation unit increases gradually in the wake of decreasing strain rate. As an improvement, different strain rates and their reciprocal regarded as coefficients are applied to the relaxation unit and creep unit of constitutive model, respectively. From the comparison between theoretical and experimental results we can see that the coefficients added to the relaxation and creep unit play a significant role in the constitutive model. Although the constitutive model has nine constants, it can be applied over a wide range of strain rates, unlike the model established by Shergold [31], which only has two coefficients, but each strain rate corresponds to a set of parameters. It can be seen that the constitutive model can fit well to the curve from about low and high strain rates as a whole. Overall, the constitutive model established by three units provides a good description of the compressive stress-versus-strain behavior of pig skin over a wide range of strain rates.

In the current study, we established a constitutive model of pig skin that is capable of describing the nonlinear visco-hyperelastic mechanical response to compression. However, this does not mean the current model is capable of describing the mechanical response under different types of loading. Actually, even the experiment taken by pig skin is uniaxial compression and the specimen is considered to be in a state of plane stress, the anisotropy of skin still has a certain impact

on the test results. Moreover, the compression experiment data obtained using pig skin might differ from other research because of the variations in test conditions and studied species. Even in the same species, the skin got from different position can also have a significant difference in mechanical properties. Hence, for the field of skin research, a full constitutive model considering the mechanical response of compression, tension and shear would be invaluable.

5. Conclusion

The parameters of the newly established constitutive model are estimated by iterative parameter estimation method. This model was able to capture the effects of relaxation, creep and strain rate under the compression mechanics response. Then, we examined the material properties of freshly harvested porcine skin in compression at strain rates from 0.01/s to 4000/s and verified this constitutive model based on the experimental results and cited data. By experimental data, it was proven that the constitutive model is universal. Good agreement between experimental results and constitutive model established to describe the compressive behavior of pig skin. However, due to the anisotropy of skin tissue, the constitutive model still needs to be improved.

Acknowledgements

This project is supported by National Natural Science Foundation of China (Grant No. 11872215 and Grant No. 11902088) and National Defense Basic Scientific Research Program of China (Grant JCKYS2019209C001).

References

[1] ANNAIDH A.N., BRUYÈRE K., DESTRADE M., GILCHRIST M.D., OTTÉNIO M., *Characterization of the anisotropic mechanical properties of excised human skin*, J. Mech. Behav. Biomed. Mater., 2012, 5 (1), 139–148.

[2] BAO Z.Y., *Study on dynamic mechanical properties of biological soft tissue*, Dissertation, Nanjing University of Science and Technology, 2019.

[3] BELFIORE L.A., *Physical properties of macromolecules*, John Wiley & Sons, 2010.

[4] BUTLER B.J., BODDY R.L., BO C., ARORA H., WILLIAMS A., PROUD W.G., BROWN K.A., *Composite nature of fresh skin revealed during compression*, Bioinsp. Biomim. Nanobiomater., 2015, 4 (2), 133–139.

[5] CHEN W., LU F., FREW D.J., FORRESTAL M.J., *Dynamic Compression Testing of Soft Material*, ASME J. Appl. Mech., 2002, 69 (3), 214–223.

[6] DE MEY J.G., CLAEYS M., VANHOUTTE P.M., *Endothelium-dependent inhibitory effects of acetylcholine, adenosine triphosphate, thrombin and arachidonic acid in the canine femoral artery*, J. Pharmacol. Exp. Ther., 1982, 222 (1), 166–173.

[7] DIMAIO V.J., COPELAND A.R., BESANT-MATTHEWS P.E., FLETCHER L.A., JONES A., *Minimal velocities necessary for perforation of skin by air gun pellets and bullets*, J. Forensic. Sci., 1982, 27 (4), 894–899.

[8] DOUGHERTY P.J., NAJIBI S., SILVERTON C., VAIDYA R., *Gunshot wounds: epidemiology, wound ballistics, and soft-tissue treatment*, Instr. Course. Lect., 2009, 58, 131–139.

[9] FACKLER M.L., *Wound ballistics and the scientific background: book review*, Wound. Ballistics. Rev., 1994, 2, 46–48.

[10] FINLAY B., *Dynamic mechanical testing of human skin "in vivo"*, J. Biomech., 1970, 3 (6), 559–568.

[11] GHORBEL-FEKI H., MASOOD A., CALIEZ M., GRATTON M., PITTET J. C., LINTS M., DOS SANTOS S., *Acousto-mechanical behaviour of ex vivo skin: Nonlinear and viscoelastic properties*, Comptes. Rendus. Mécanique., 2019, 347 (3), 218–227.

[12] GROVES R.B., COULMAN S.A., BIRCHALL J.C., EVANS S.L., *An anisotropic, hyperelastic model for skin: experimental measurements, finite element modelling and identification of parameters for human and murine skin*, J. Mech. Behav. Biomed. Mater., 2013, 18, 167–180.

[13] HAUT R.C., *The effects of orientation and location on the strength of dorsal rat skin in high and low speed tensile failure experiments*, J. Biomech. Eng., 1989, 111, 136–140.

[14] HOLT B., TRIPATHI A., MORGAN J., *Viscoelastic response of human skin to low magnitude physiologically relevant shear*, J. Biomech., 2008, 41 (12), 2689–2695.

[15] KARIMI A., FATURECHI R., NAVIDBAKHSH M., HASHEMI S.A., *A non-linear hyperelastic behavior to identify the mechanical properties of rat skin under uniaxial loading*, J. Mech. Med. Biol., 2014, 14 (5), 1–14.

[16] KOENE L., PAPY A., *Towards a better, science-based, evaluation of kinetic non-lethal weapons*, Int. J. Intelligent. Defence. Support. Systems., 2011, 4 (2), 169–186.

[17] ŁAGAN S.D., LIBER-KNEĆ A., *Experimental testing and constitutive modeling of the mechanical properties of the swine skin tissue*. Act. Bioeng. Biomech., 2017, 19 (2), 93–102.

[18] LAMERS E., VAN KEMPEN T.H.S., BAAIJENS F.P.T., PETERS G.W.M., OOMENS C.W.J., *Large amplitude oscillatory shear properties of human skin*, J. Mech. Behav. Biomed. Mater., 2013, 28, 462–470.

[19] LANIR Y., FUNG Y.C., *Two-dimensional mechanical properties of rabbit skin – I. Experimental system*, J. Biomech., 1974, 7, 29–34.

[20] LAPEER R.J., GASSON P.D., KARRI V., *Simulating plastic surgery: From human skin tensile tests, through hyperelastic finite element models to real-time haptics*, Prog. Biophys. Mol. Bio., 2010, 103 (2–3), 208–216.

[21] LI W., LUO X.Y., *An Invariant-Based Damage Model for Human and Animal Skins*, Ann. Biomed. Eng., 2016, 44, 3109–3122.

[22] LIM J., HONG J., CHEN W.W., WEERASOORIYA T., *Mechanical response of pig skin under dynamic tensile loading*, Int. J. Impact. Eng., 2011, 38 (2), 130–135.

[23] LIU K., WU Z.L., REN H.L., LI Z.X., NING J.G., *Strain rate sensitive compressive response of gelatine: Experimental and constitutive analysis*, Polym. Testing., 2017, 6, 254–266.

[24] MISSLIWETZ J., *Critical velocity in skin (an experimental ballistic study with firearms of 4 mm and 4.5 mm calibers)*, Beitr. Gerichtl. Med., 1987, 45, 411–432.

[25] NICOLLE S., DECORPS J., FROMY B., PALIERNE J.-F., *New regime in the mechanical behavior of skin: strain-softening occurring before strain-hardening*, J. Mech. Behav. Biomed. Mater., 2017, 69, 98–106.

[26] PISSARENKO A., MEYERS M.A., *The materials science of skin: Analysis, characterization, and modeling*, Prog. Mater. Sci., 2020, 110, 100634.

[27] REIHSNER R., MENZEL E.J., *Two-dimensional stress–relaxation behavior of human skin as influenced by non-enzymatic glycation and the inhibitory agent aminoguanidine*, J. Biomech., 1998, 31 (11), 985–993.

[28] RIDGE M.D., WRIGHT V., *The directional effects of skin*, J. Invest. Dermatol., 1965, 46, 341–6.

[29] RUBIN M.B., BODNER S.R., BINUR N.S., *An elastic-viscoplastic model for excised facial tissues*, J. Biomech. Eng., 1998, 120 (5), 686–689.

[30] SCHNEIDER D.C., DAVIDSON T.M., NAHUM A.M., *In vitro biaxial stress–strain response of human skin*, Arch. Otolaryngol., 1984, 110 (5), 329–333.

[31] SHERGOLD O.A., FLECK N.A., RADFORD D., *The uniaxial stress versus strain response of pig skin and silicone rubber at low and high strain rates*, Int. J. Impact. Eng., 2006, 32 (9), 1384–1402.

[32] SOETENS J.F.J., VAN VIJVEN M., BADER D.L., PETERS G.W.M., OOMENS C.W.J., *A model of human skin under large amplitude oscillatory shear*, J. Mech. Behav. Biomed. Mater., 2018, 86, 423–432.

[33] TAUSCH D., SATTLER W., WEHRFRITZ K., WEHRFRITZ G., WAGNER H.J., *Experiments on the penetration power of various bullets into skin and muscle tissue*, Z. Rechtsmed., 1978, 81 (4), 309–328.

[34] WEISS J.A., MAKER B.N., GOVINDJEE S., *Finite element implementation of incompressible, transversely isotropic hyperelasticity*, Comput. Meth. Appl. Mech. Eng., 1996, 135, 107–128.

[35] WU J.Z., DONG R.G., SMUTZ P., SCHOPPER A.W., *Nonlinear and Viscoelastic Characteristics of Skin Under Compression: Experiment and Analysis*, Biomed. Mater. Eng., 2003, 13 (4), 373–385.